Appendix to:
C.A.J. Appelo, Principles, caveats and improvements in databases for calculating hydrogeochemical reactions in saline waters from 0 - 200 ºc and 1 - 1000 atm.

This appendix has figures showing experimental solubilities and PHREEQC calculations, using the Pitzer interaction coefficients given in Table 1, and the temperature dependent log *K*'s in Table 2 of the paper. The PHREEQC input files can be downloaded as zip from:
http://www.hydrochemistry.eu/pub/pitzer_db/appendix.zip
Extract the file in your computer. The main directory contains pitzer.dat and input files that calculate the figures presented by Pabalan and Pitzer, 1987. Input files for other minerals and $CO_2$ gas are in sub-directories.
It is easiest to run the files with Notepad++ adapted for PHREEQC. Download from:
http://www.hydrochemistry.eu/ph3/phreeqc3.Installer.exe
and install in your computer. In Notepad++, open a file (Ctrl+O), and press Ctrl+F6 to start the PHREEQC calculations.

Table 3. List of figures with mineral solubilities as a function of *T, P* and solution composition.

| Mineral solubility in water or aqueous solution | Temp ºC | Pressure / atm | Figure |
|---|---|---|---|
| halite (NaCl) | 0 - 300 | 1 - $P_{sat}$ | A1 |
| sylvite (KCl) | 10 - 300 | 1 - $P_{sat}$ | A2 |
| bischofite ($MgCl_2$:6$H_2O$), $MgCl_2$:2$H_2O$, $MgCl_2$:4$H_2O$ | 0 - 200 | 1 - $P_{sat}$ | A3 |
| mirabilite ($Na_2SO_4$:10$H_2O$), thenardite ($Na_2SO_4$) | 0 - 220 | 1 - $P_{sat}$ | A4 |
| arcanite ($K_2SO_4$) | 0 - 210 | 1 - $P_{sat}$ | A5 |
| epsomite ($MgSO_4$:7$H_2O$), hexahydrite ($MgSO_4$:6$H_2O$), kieserite ($MgSO_4$:$H_2O$) | 0 - 200 | 1 - $P_{sat}$ | A6 |
| halite (NaCl), sylvite (KCl) in Na/K-Cl solutions | 0 - 200 | 1 - $P_{sat}$ | A7 |
| carnallite ($KMgCl_3$:$H_2O$) in K/Mg-Cl solutions | 0 - 75 | 1 | A8 |
| gypsum ($CaSO_4$:2$H_2O$) | 0 - 95 | 1 | A9 |
| gypsum ($CaSO_4$:2$H_2O$) in NaCl solutions | 0.5 - 95 | 1 | A10 |
| gypsum ($CaSO_4$:2$H_2O$), mirabilite ($Na_2SO_4$:10$H_2O$), glauberite ($Na_2Ca(SO_4)_2$) and thenardite ($Na_2SO_4$) in $Na_2SO_4$ solutions | 25 - 100 | 1 | A11 |
| gypsum ($CaSO_4$:2$H_2O$) and anhydrite ($CaSO_4$) | 30 - 160 | 1 - 1000 | A12 |
| anhydrite ($CaSO_4$) in NaCl solutions | 100 - 200 | 1 - $P_{sat}$ | A13 |
| anhydrite ($CaSO_4$) in NaCl solutions | 100 - 200 | 1 - 987 | A14 |
| anhydrite ($CaSO_4$) and glauberite ($Na_2Ca(SO_4)_2$) in $Na_2SO_4$ solutions | 100 - 200 | 1 - $P_{sat}$ | A15 |
| anhydrite ($CaSO_4$), Goergeyite ($K_2Ca_5(SO_4)_6H_2O$) and syngenite ($K_2Ca(SO4)_2$:$H_2O$) in $K_2SO_4$ solutions | 100 - 200 | 1 - $P_{sat}$ | A16 |
| amorphous silica ($SiO_2$(a)) in NaCl solutions | 25 - 300 | 1 - $P_{sat}$ | A17 |
| amorphous silica ($SiO_2$(a)) in $Na_2SO_4$ solutions | 25 - 300 | 1 - $P_{sat}$ | A18 |
| amorphous silica ($SiO_2$(a)) in $MgCl_2$ solutions | 25 - 300 | 1 - $P_{sat}$ | A19 |
| amorphous silica ($SiO_2$(a)) in $MgSO_4$ solutions | 25 - 250 | 1 - $P_{sat}$ | A20 |
| amorphous silica ($SiO_2$(a)) in Li-Cl/$NO_3$ solutions | 25 | 1 | A21 |

| | | | |
|---|---|---|---|
| amorphous silica ($SiO_2$(a)) in K-Cl/$NO_3$ solutions | 25 | 1 | A22 |
| amorphous silica ($SiO_2$(a)) in $CaCl_2$ solutions | 25 | 1 | A23 |
| barite ($BaSO_4$) in NaCl solutions | 1 - 250 | 1 - $P_{sat}$ | A24 |
| barite ($BaSO_4$) in NaCl solutions | 150 - 250 | 493 | A25 |
| calcite ($CaCO_3$) in NaCl solutions | 10 - 60 | 1 | A26 |
| calcite ($CaCO_3$) in 3 M NaCl, variable $CO_2$ | 200 | 580 | A27 |
| calcite ($CaCO_3$) in NaCl solutions | 120 - 260 | 12 | A28 |
| calcite ($CaCO_3$) at 1 bar $CO_2$ pressure | 0 - 300 | 1 - ($P_{sat}$+1) | A29 |
| calcite ($CaCO_3$) in NaCl solutions at 1 bar $CO_2$ pressure | 0 - 250 | 1 - 1450 | A30 |
| $CO_2$ gas | 25 - 100 | 1 - 710 | A31 |
| $CO_2$ gas in 1 and 6 M NaCl solution | 25 - 300 | 35 - 200 | A32 |
| $CO_2$ gas in 4 M NaCl solution | 80 - 180 | 9 - 95 | A33 |
| $CO_2$ gas in $Na_2SO_4$ solutions | 140 | 12 - 96 | A34 |
| $CO_2$ gas in 2.3 M $CaCl_2$ solution | 75 - 120 | 22 - 655 | A35 |
| $CO_2$ fugacity coefficients | 0 - 300 | 99 - 987 | A36 |

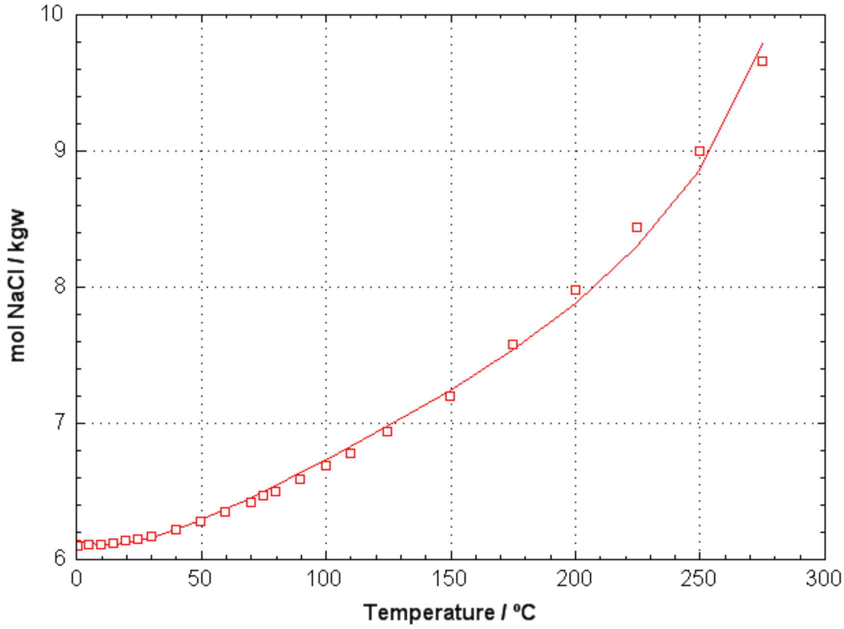


Figure A1. Halite (NaCl) solubility as a function of temperature. Data points from Pabalan and Pitzer, 1987; Clarke and Glew, 1985. File Halite.phr

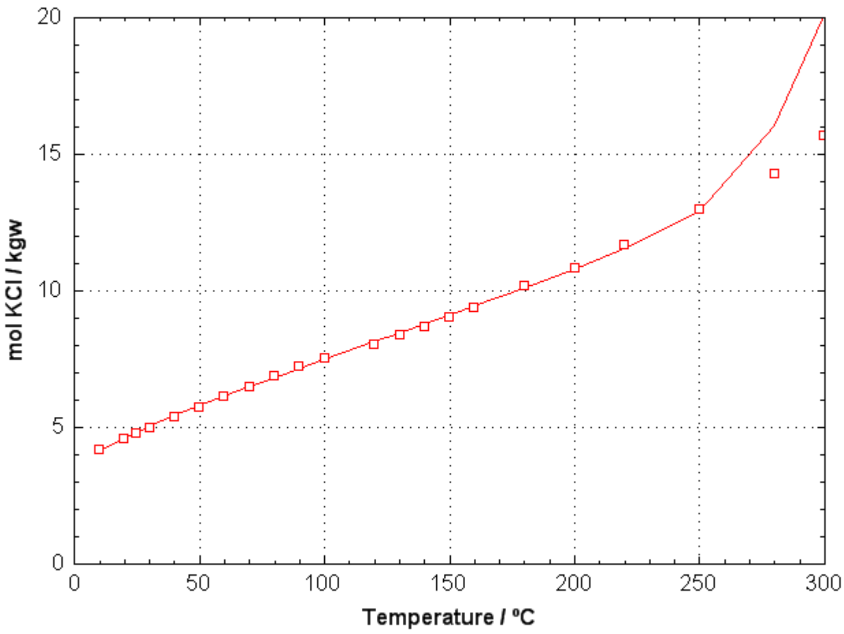


Figure A2. Sylvite (KCl) solubility as a function of temperature. Data points from Pabalan and Pitzer, 1987. File Sylvite.phr

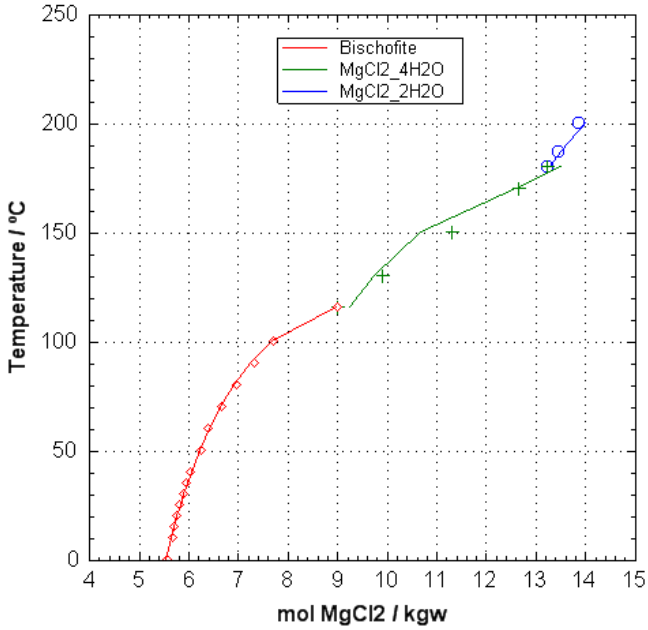


Figure A3. Solubility of $MgCl_2$-hydrates. Data points from Pabalan and Pitzer, 1987. File $MgCl_2$.phr

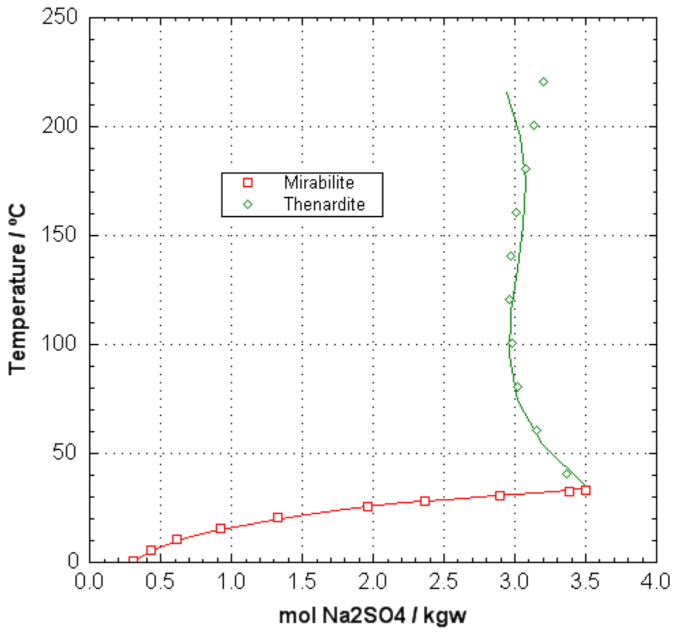


Figure A4. Solubility of $Na_2SO_4$-(an)hydrate. Data points from Pabalan and Pitzer, 1987. File Na2SO4.phr

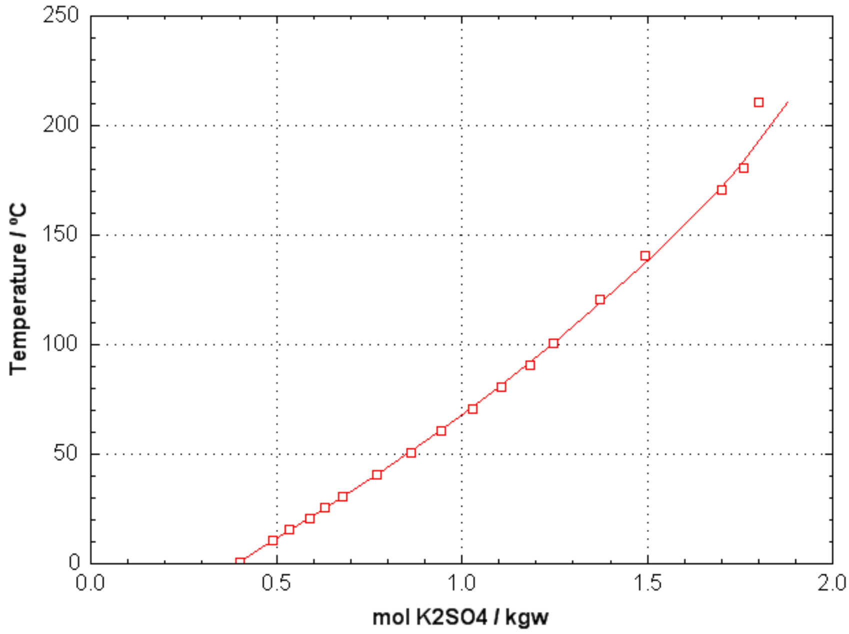


Figure A5. Solubility of arcanite ($K_2SO_4$). Data points from Pabalan and Pitzer, 1987. File K2SO4.phr

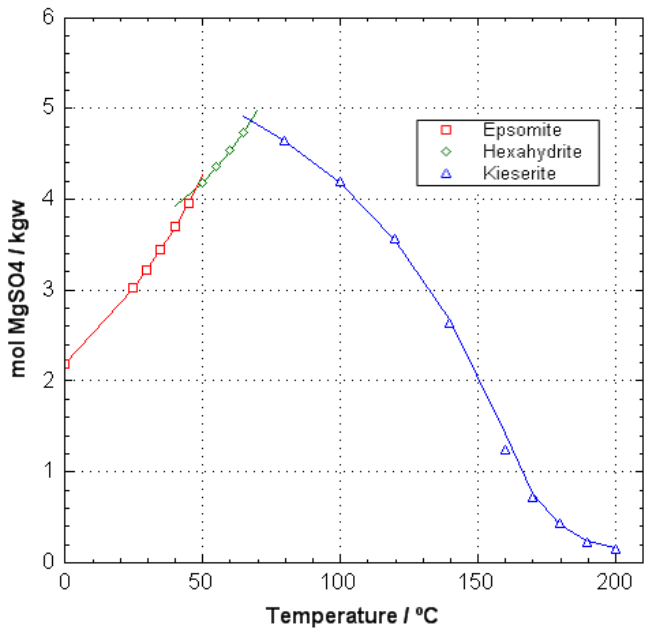


Figure A6. Solubility of $MgSO_4$-hydrates. Data points from Pabalan and Pitzer, 1987. File MgSO4.phr

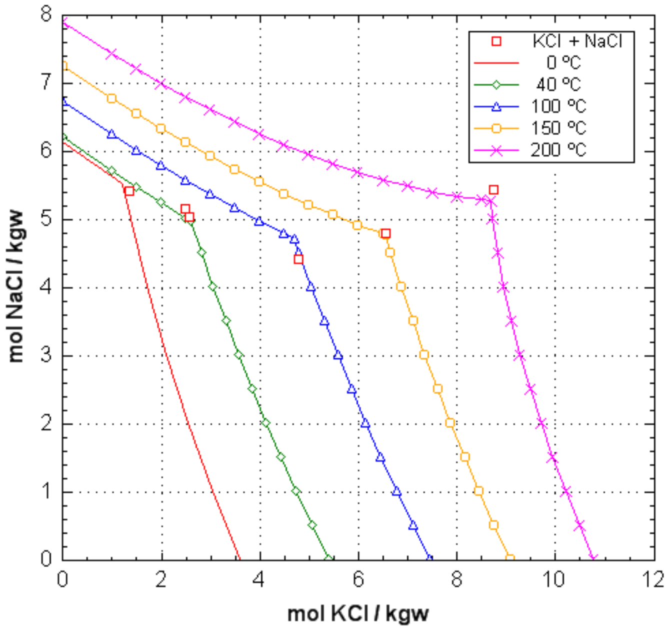


Figure A7. Mutual influence of NaCl and KCl solutions on halite and sylvite solubilities, with triple points KCl + NaCl + $H_2O$ from Pabalan and Pitzer, 1987. File NaKCl.phr

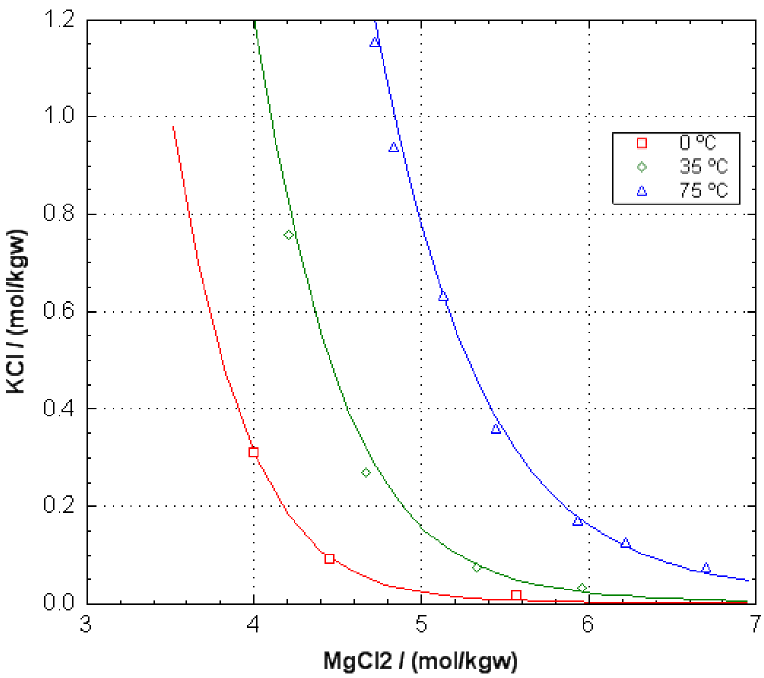


Figure A8. Solubility of carnallite ($KMgCl_3$:$H_2O$). Data points from Pabalan and Pitzer, 1987. File Carnallite.phr

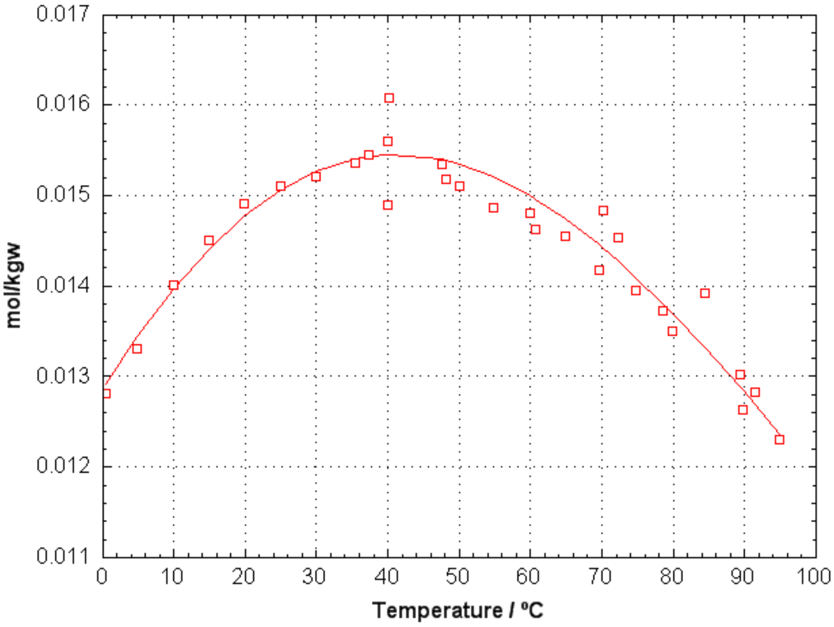


Figure A9. Solubility of gypsum ($CaSO_4$:$2H_2O$). Data points from Marshall and Slusher, 1966; Blount and Dickson, 1969. File gypsum.phr

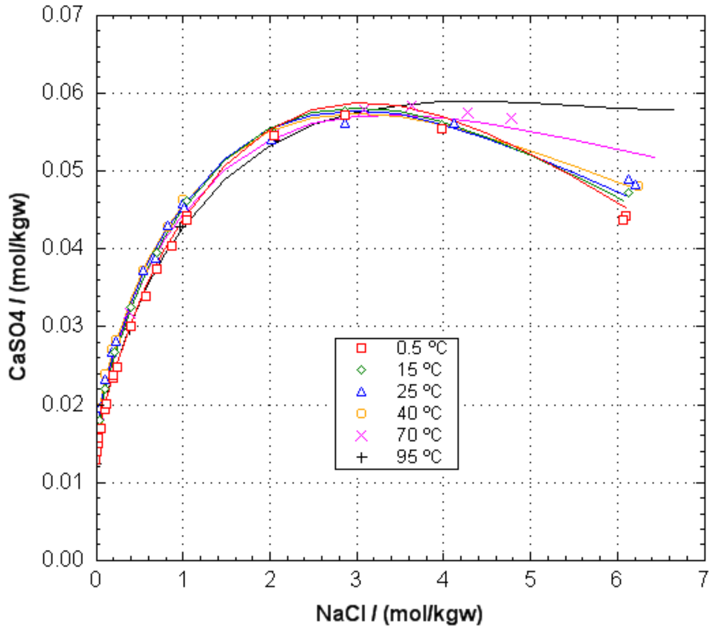


Figure A10. Solubility of gypsum ($CaSO_4$:$2H_2O$) in NaCl solutions. Data points from Marshall and Slusher, 1966. File gyps_NaCl.phr

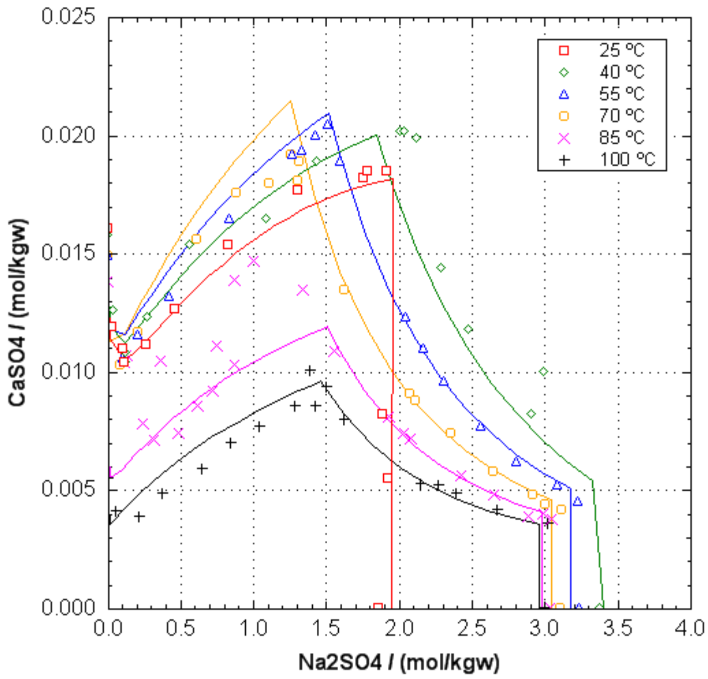


Figure A11. Solubility of gypsum ($CaSO_4$•$2H_2O$) in $Na_2SO_4$ solutions. Data points from Block and Waters, 1968. File gyps_Na2SO4.phr. The concentration decrease of $CaSO_4$ at $Na_2SO_4$ concentrations above 1 M is due to mirabilite precipitation (25ºC), or glauberite and thenardite precipitation at higher temperatures. At 85 and 100ºC, and possibly at 70ºC, gypsum transforms into anhydrite.

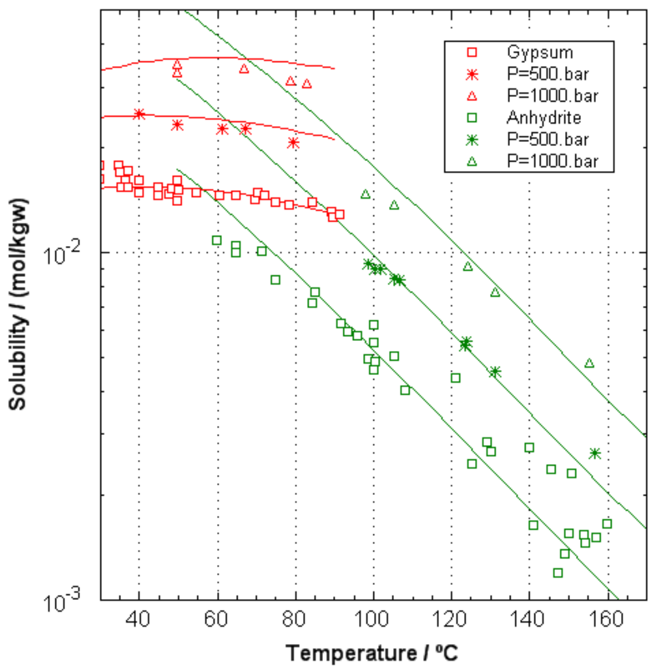


Figure A12. Solubility of gypsum ($CaSO_4$•$2H_2O$) and anhydrite ($CaSO_4$) as a function of temperature and pressure. Data points from Blount and Dickson, 1973. File gypsum_P.phr.

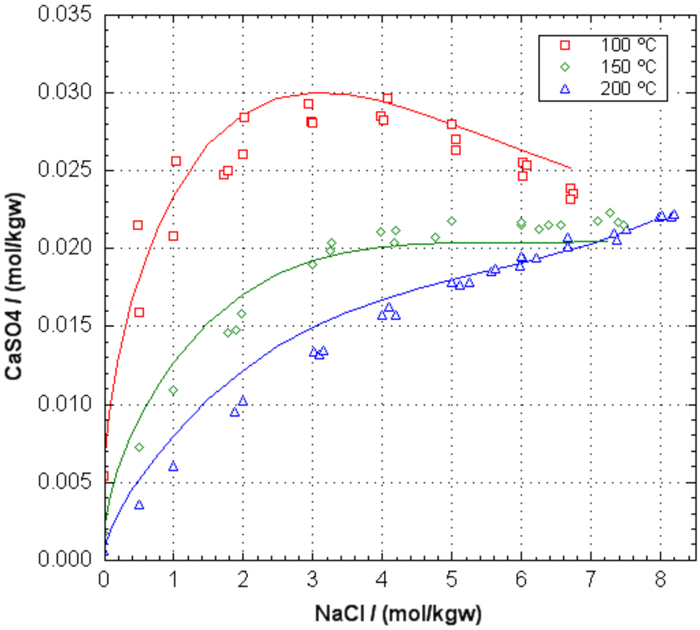


Figure A13. Solubility of anhydrite ($CaSO_4$) in NaCl solutions. Data points from Block and Waters, 1968; Blount and Dickson, 1969; Freyer and Voigt, 2004. File anhy_NaCl.phr.

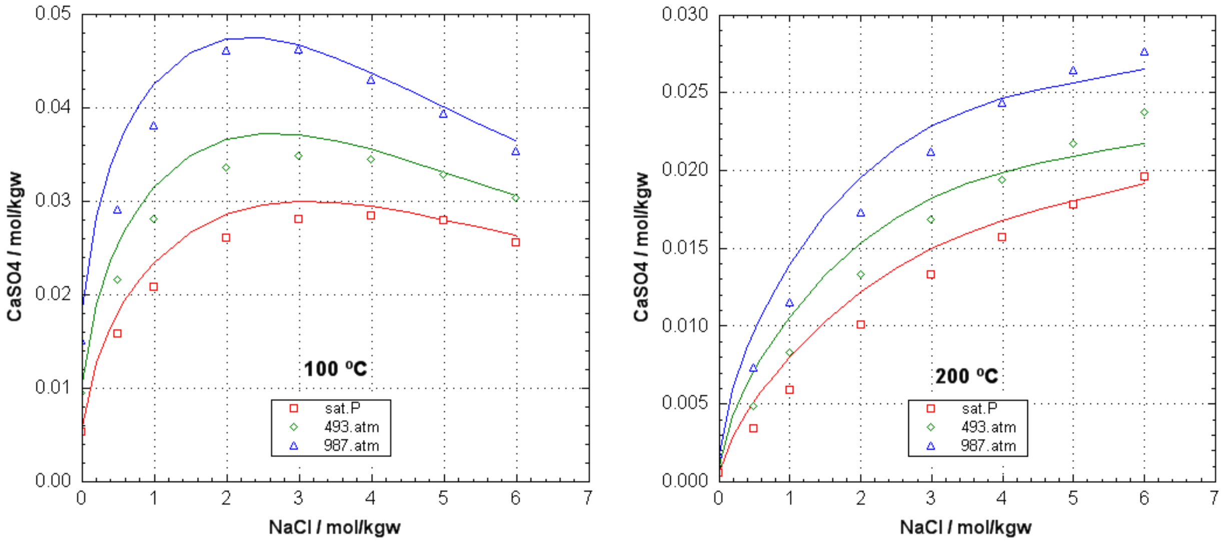


Figure A14. Solubility of anhydrite ($CaSO_4$) in NaCl solutions as a function of pressure at 100ºC and 200ºC. Data points from the summary table in Blount and Dickson, 1969. File anhy_P_NaCl.phr.

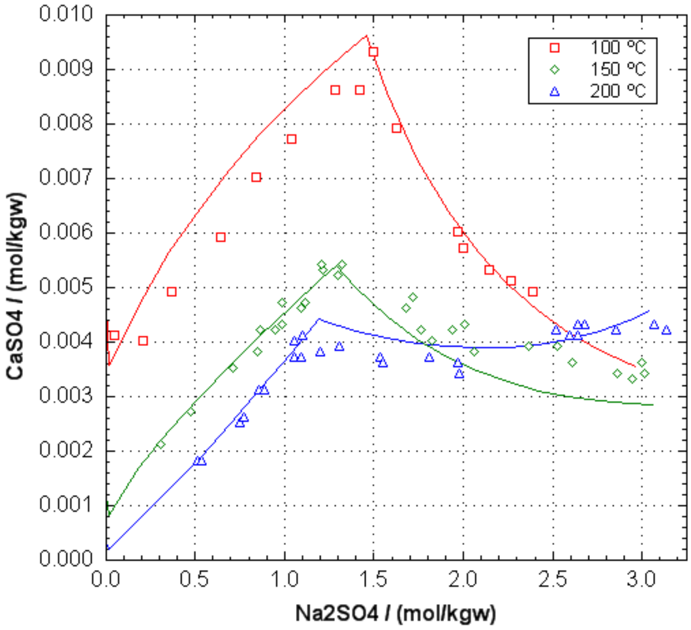


Figure A15. Solubility of anhydrite ($CaSO_4$) in $Na_2SO_4$ solutions. Data points from Freyer and Voigt, 2004. The decrease of the $CaSO_4$ concentration at $Na_2SO_4$ concentrations above 1 M is due to glauberite precipitation. File anhy_Na2SO4.phr.

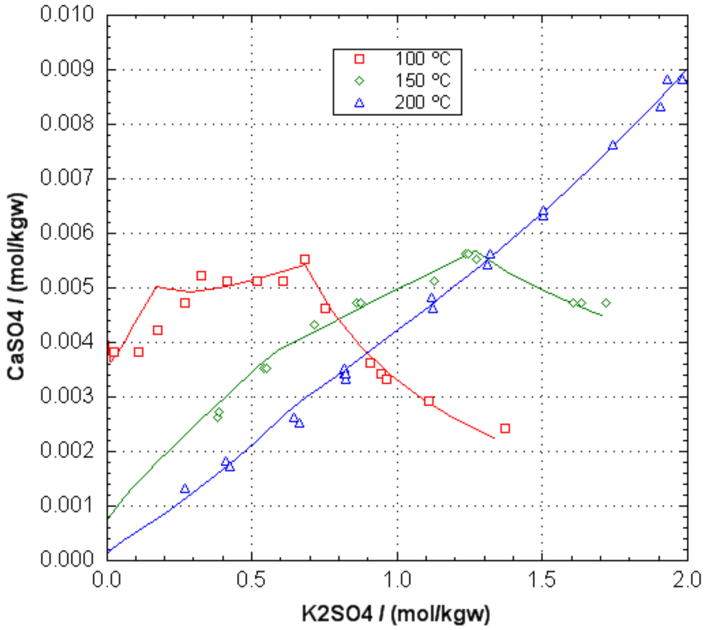


Figure A16. Solubility of anhydrite ($CaSO_4$) in $K_2SO_4$ solutions. Data points from Freyer and Voigt, 2004. The breaks in the concentration lines result from precipitation of Goergeyite ($K_2Ca_5(SO_4)_6H_2O$) and, at 100 and 150ºC, Syngenite ($K_2Ca(SO4)_2$:$H_2O$). File anhy_K2SO4.phr.

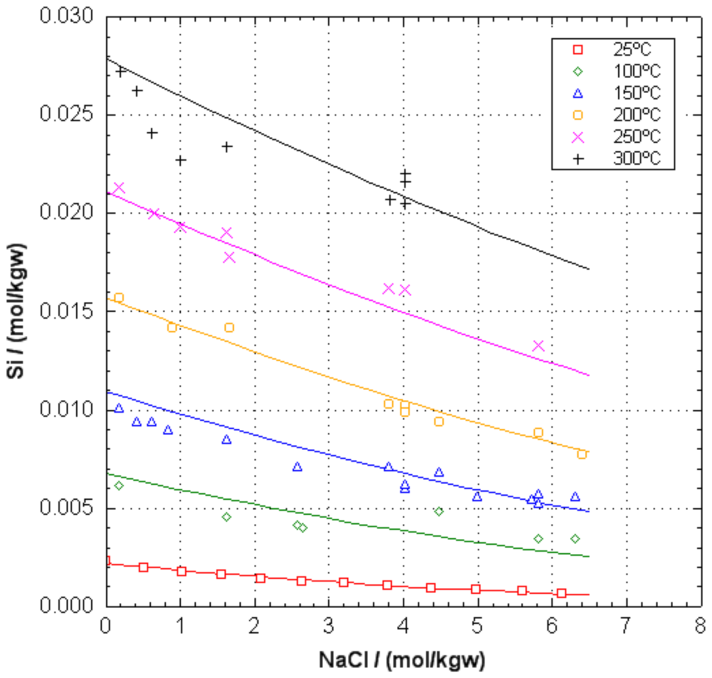

Figure A17. Solubility of amorphous silica ($SiO_2$(a)) in NaCl solutions. Data points from Marshall and Warakomski, 1980, and Chen and Marshall, 1982. File SiO2_NaCl.phr.

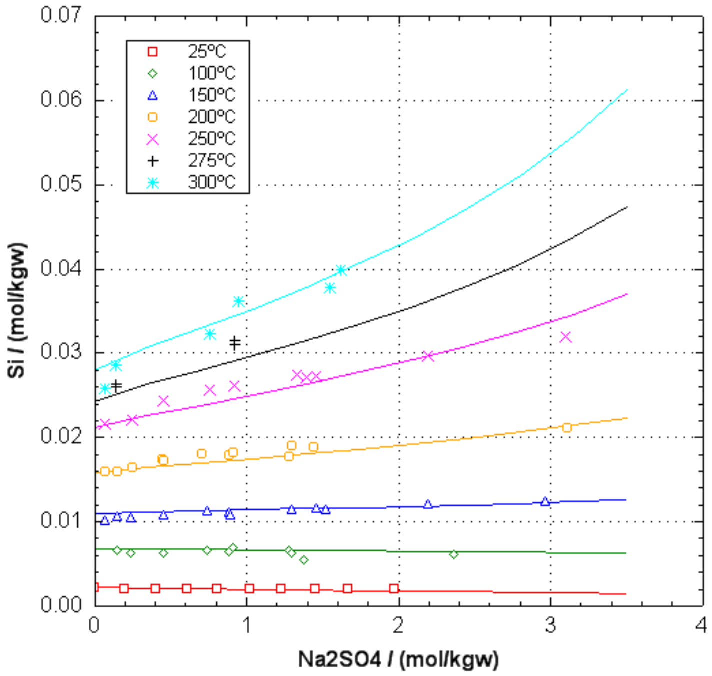

Figure A18. Solubility of amorphous silica ($SiO_2$(a)) in $Na_2SO_4$ solutions. Data points from Marshall and Warakomski, 1980, and Chen and Marshall, 1982. File SiO2_Na2SO4.phr.

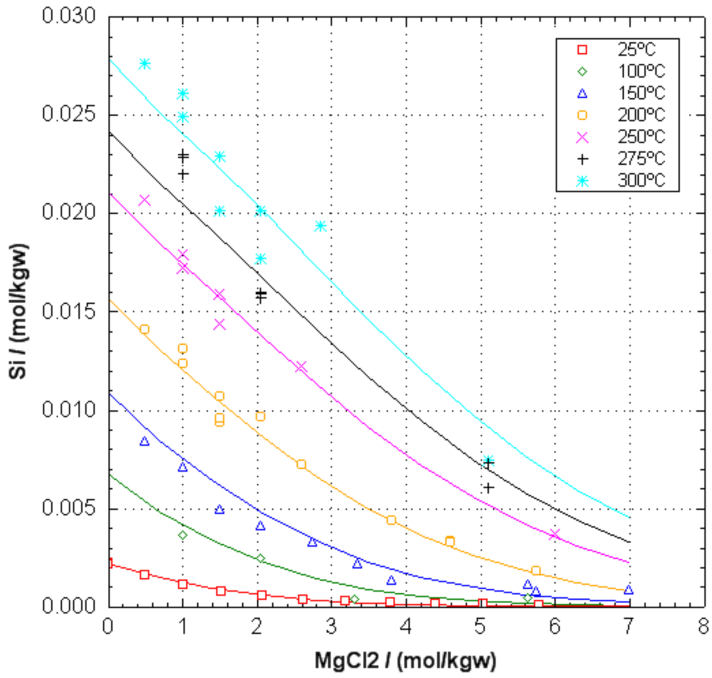


Figure A19. Solubility of amorphous silica ($SiO_2$(a)) in $MgCl_2$ solutions. Data points from Marshall and Warakomski, 1980, and Chen and Marshall, 1982. File SiO2_ MgCl2.phr.

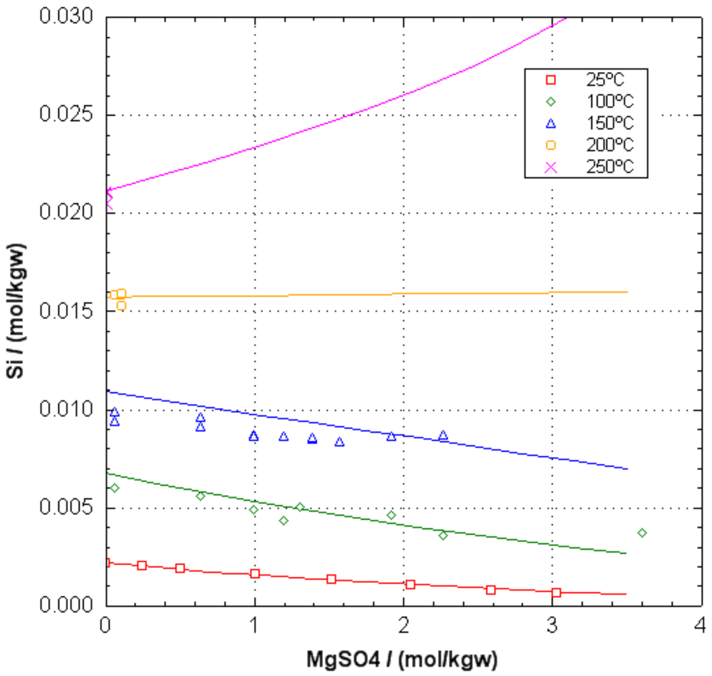


Figure A20. Solubility of amorphous silica ($SiO_2$(a)) in $MgSO_4$ solutions. Data points from Marshall and Warakomski, 1980, and Chen and Marshall, 1982. File SiO2_MgSO4.phr.

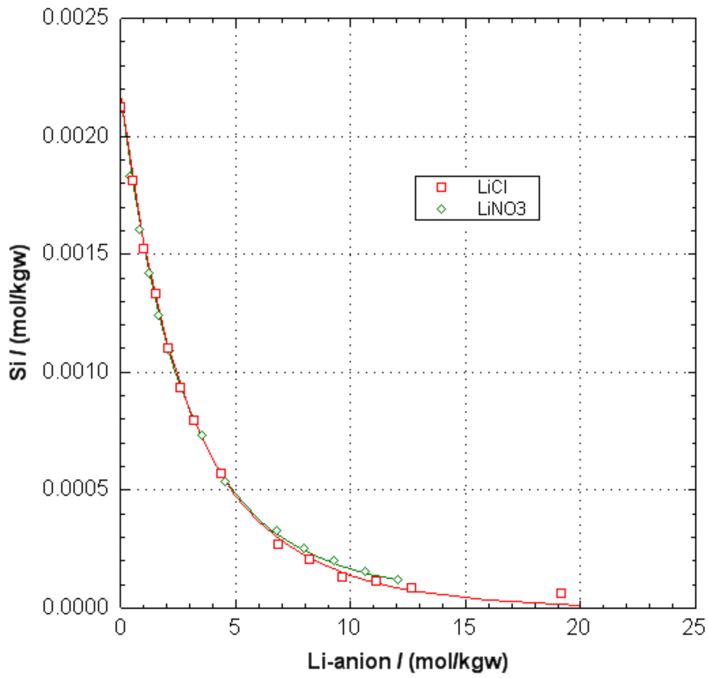


Figure A21. Solubility of amorphous silica ($SiO_2$(a)) in LiCl and $LiNO_3$ solutions at 25ºC. Data points from Marshall and Warakomski, 1980. File SiO2_Li.phr.

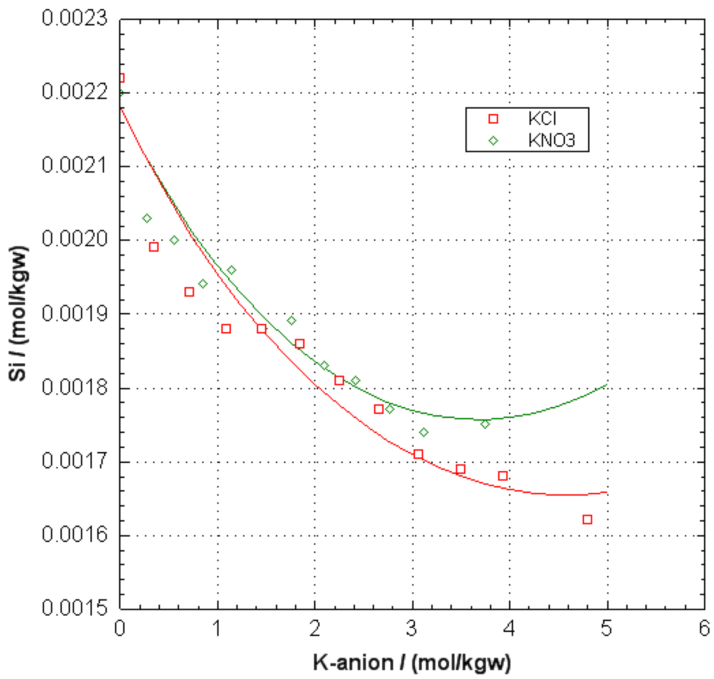


Figure A22. Solubility of amorphous silica ($SiO_2$(a)) in KCl and $KNO_3$ solutions at 25ºC. Data points from Marshall and Warakomski, 1980. File SiO2_K.phr.

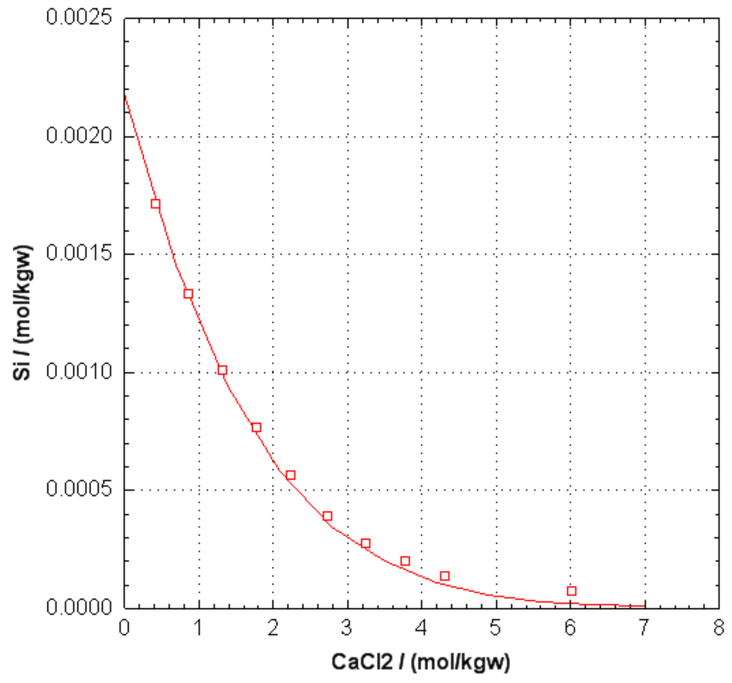


Figure A23. Solubility of amorphous silica ($SiO_2(a)$) in $CaCl_2$ solutions at 25ºC. Data points from Marshall and Warakomski, 1980. File SiO2_CaCl2.phr.

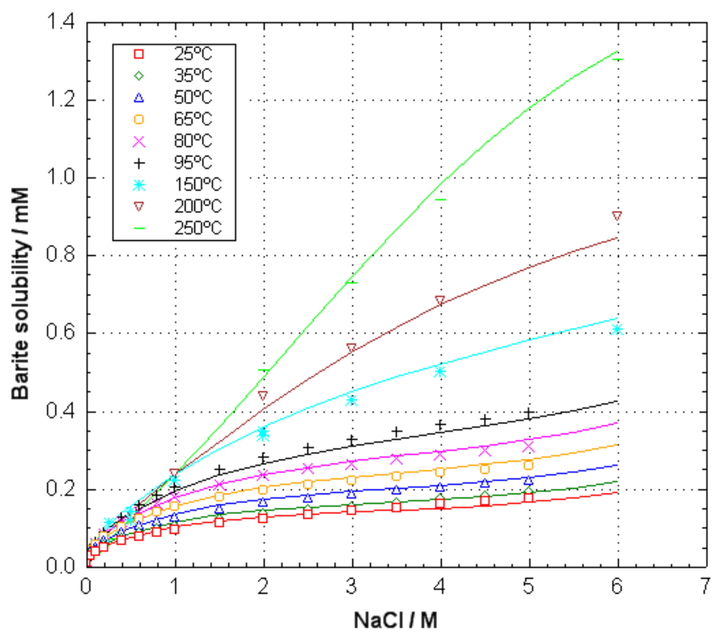


Figure A24. Solubility of barite ($BaSO_4$) in NaCl solutions. Data points < 95ºC from Templeton, 1960, > 100ºC from Uchameyshvili et al., 1966, and the summary table in Blount, 1977. File Barite_NaCl.phr.

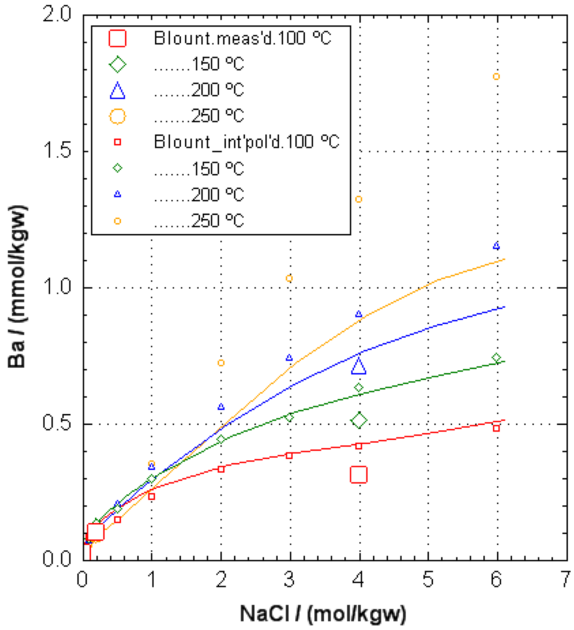


Figure A25. Solubility of barite ($BaSO_4$) in NaCl solutions at 500 bar. Measured (large symbols) and interpolated (small symbols) data from Blount, 1977. File Barite_500.phr.

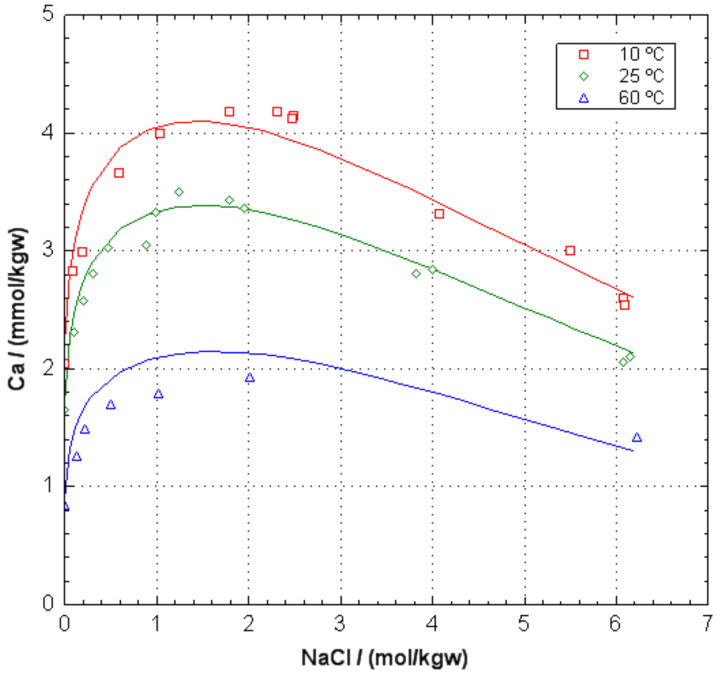


Figure A26. Solubility of calcite ($CaCO_3$) in NaCl solutions at about 0.01 atm $CO_2$ pressure. Measured data from Wolf et al., 1989. File cc_Wolf.phr.

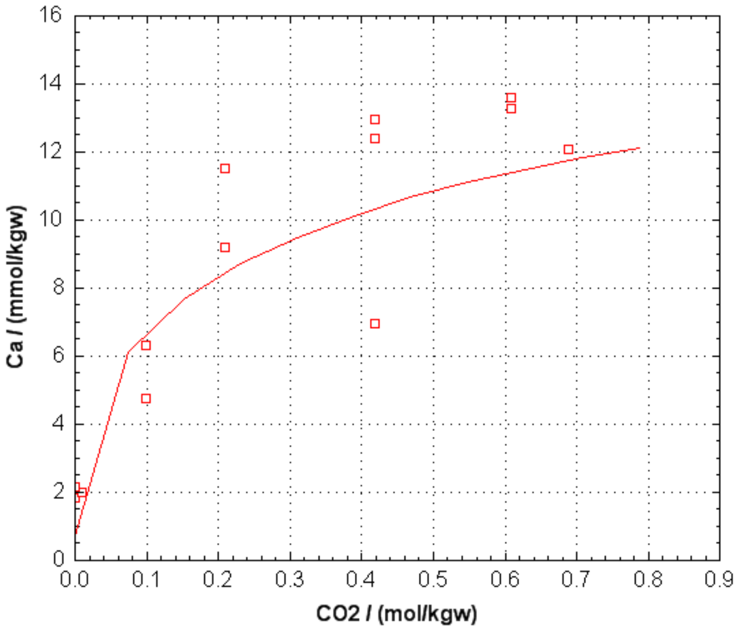


Figure A27. Solubility of calcite ($CaCO_3$) at 200 °C, 580 atm pressure in 3 M NaCl as a function of the $CO_2$ concentration. Measured data from Malinin and Kanukov, 1971. File cc_Malin.phr.

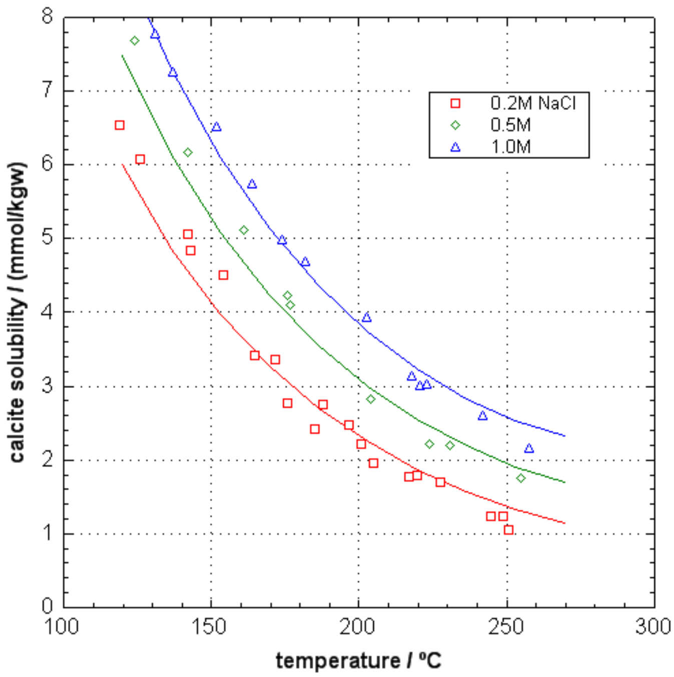


Figure A28. Solubility of calcite ($CaCO_3$) in NaCl solutions at 12 bar $CO_2$ pressure. Measured data from Ellis, 1963. File cc_Ellis.phr.

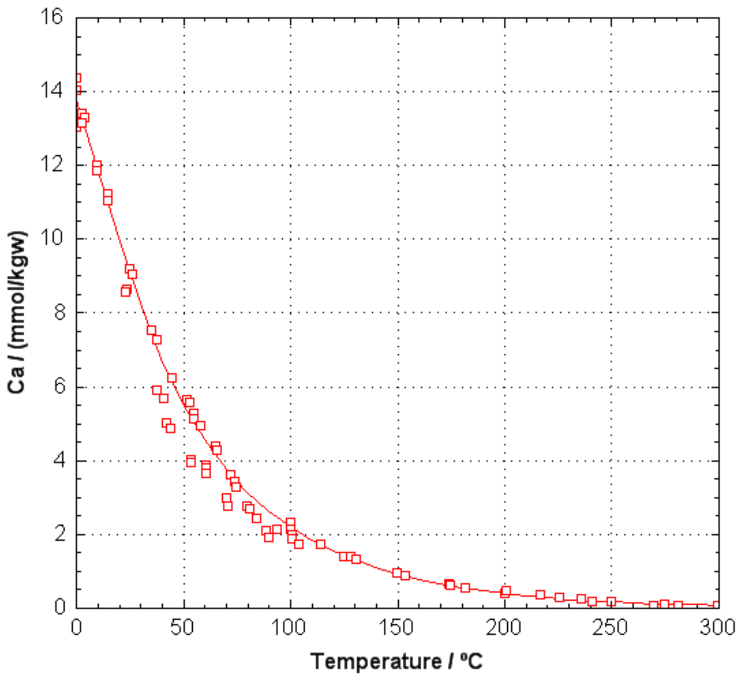


Figure A29. Solubility of calcite ($CaCO_3$) as a function of temperature at 1 bar $CO_2$ pressure. Measured data from Miller, 1952; Ellis, 1959; Plummer and Busenberg, 1982. File cc_1barCO2.phr.

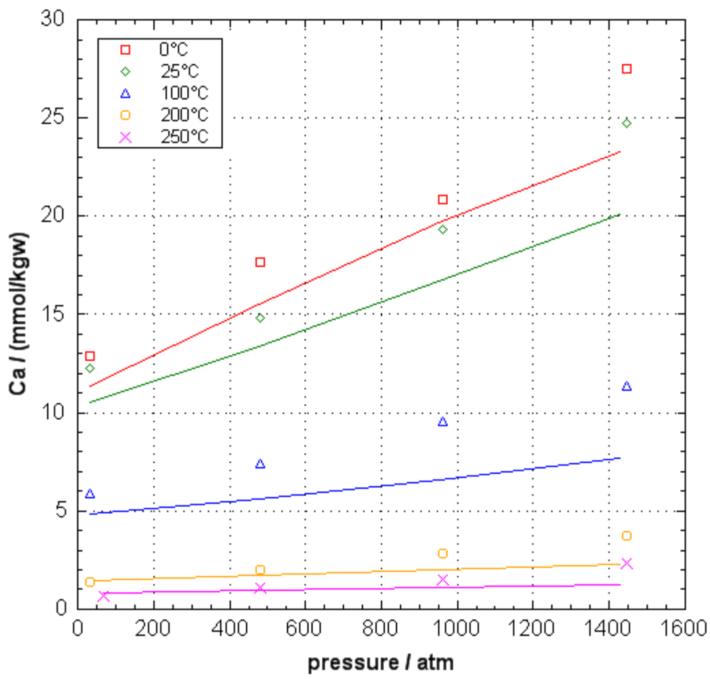


Figure A30. Solubility of calcite ($CaCO_3$) in 0.1 M NaCl as a function of temperature and pressure at 1 bar $CO_2$ pressure. Measured data from Shi et al., 2013. File cc_Shi.phr. Solubilities at 4 M NaCl and in a brine are also calculated when the file is run.

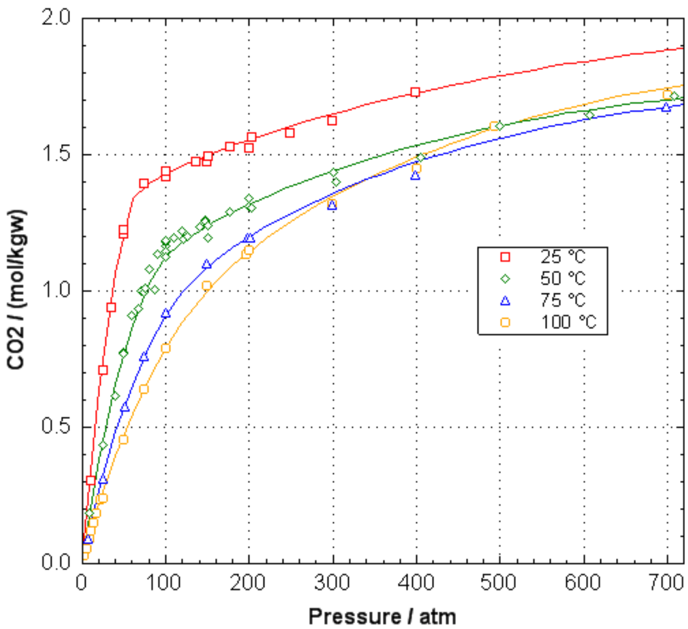


Figure A31. Solubility of $CO_2$ gas in water. Measured data from Wiebe and Gaddy, 1939, 1940; King et al., 1992; Takenouchi and Kennedy, 1964. File CO2_conc_PR_IS.phr.

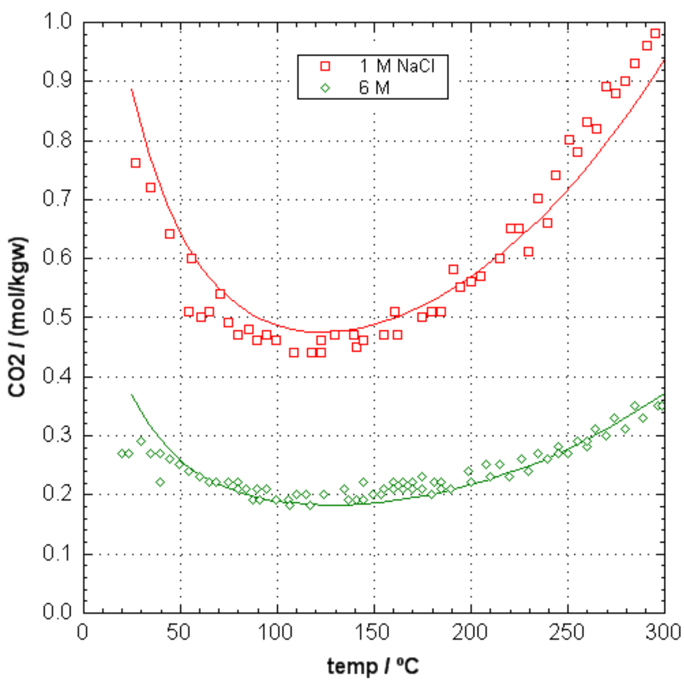


Figure A32. Solubility of $CO_2$ gas in 1 and 6 M NaCl solutions at about 40 atm $CO_2$. Measured data from Drummond, 1981. File Drummond.phr.

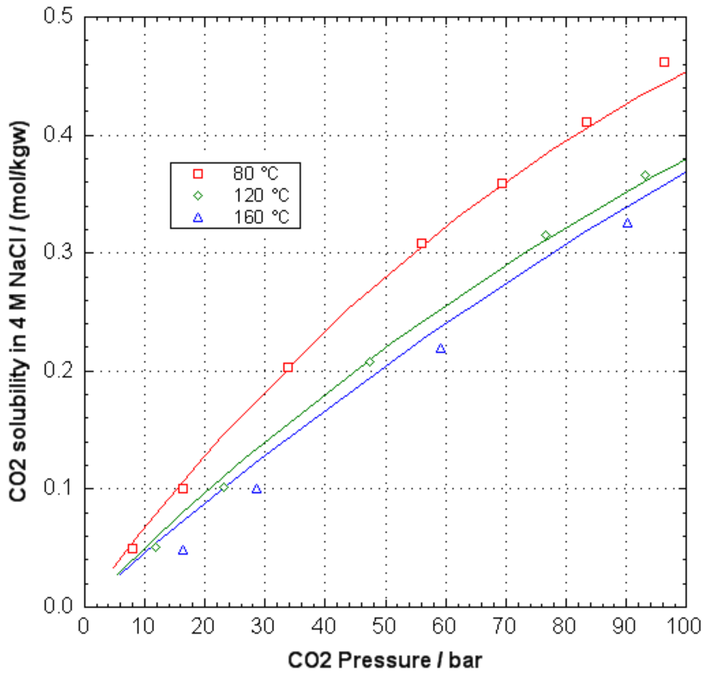


Figure A33. Solubility of $CO_2$ gas in 4 M NaCl solution. Measured data from Rumpf et al. 1994. File CO2_4M_NaCl.phr.

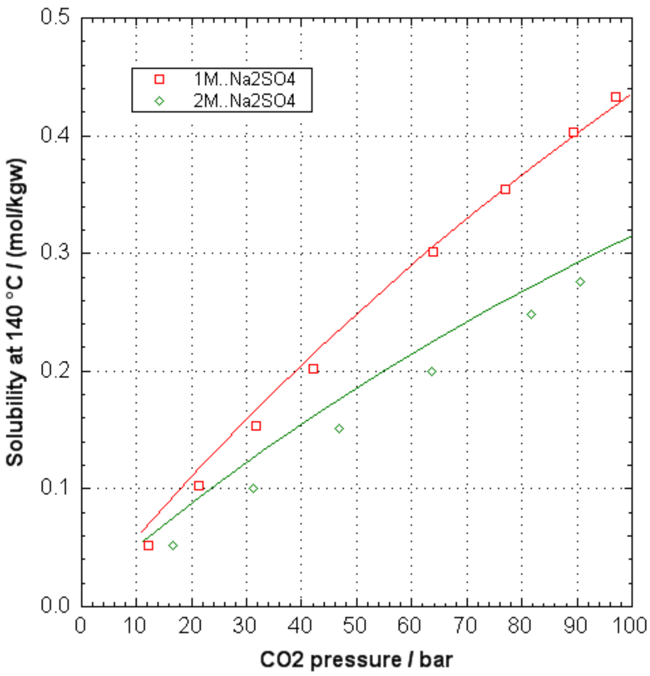


Figure A34. Solubility of $CO_2$ gas in $Na_2SO_4$ solutions at 140ºC. Measured data from Rumpf and Maurer, 1993. File P_CO2_Na2SO4.phr.

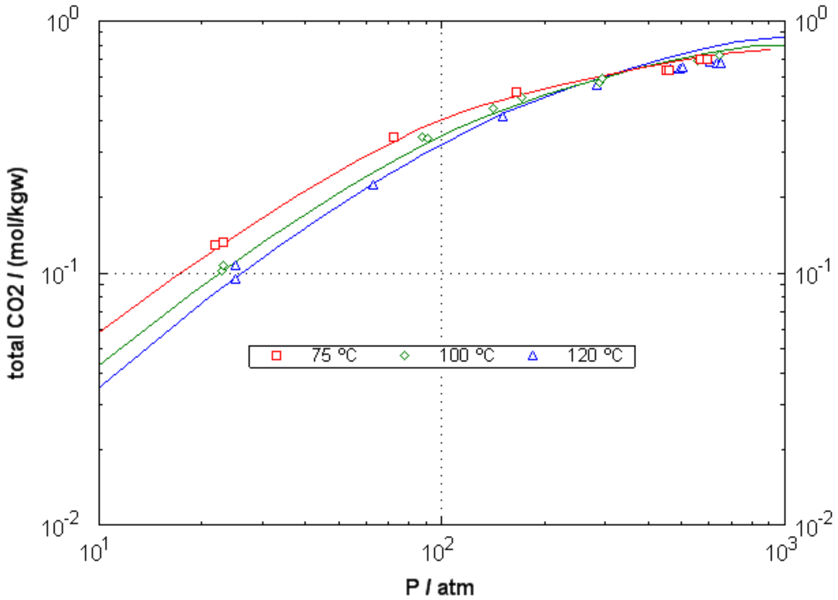


Figure A35. Solubility of $CO_2$ gas in 2.3 M $CaCl_2$ solution. Data from Springer et al., 2012. File CO2_CaCl2.phr.

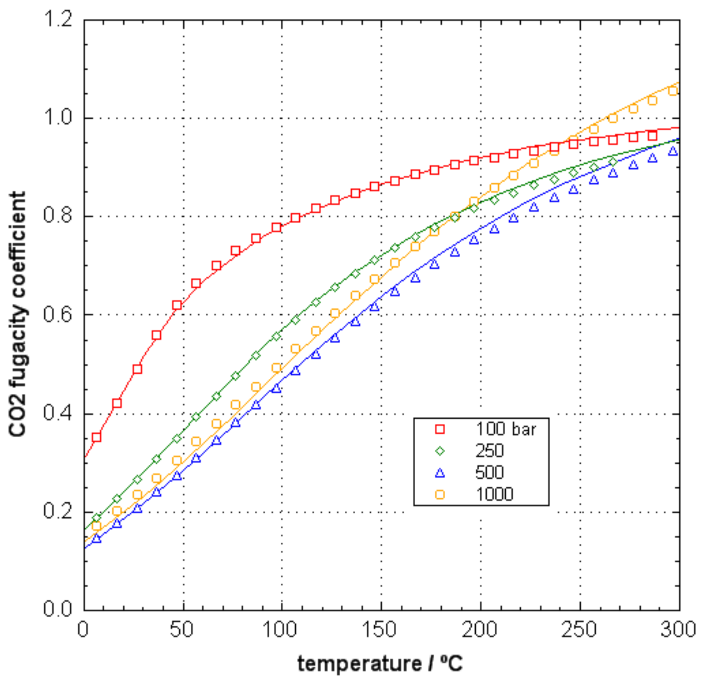


Figure A36. $CO_2$ fugacity coefficient as a function of temperature for $CO_2$ gas pressures from 100 - 1000 bar. Data from Angus et al., 1976. File phi_Angus_bar.phr.